Electronic structure around a vortex core in iron pnictide superconductors

Da Wang, Jian Xu, Yuan-Yuan Xiang, and Qiang-Hua Wang*
National Laboratory of Solid State Microstructures and Department of Physics, Nanjing University, Nanjing 210093, China
(Received 25 May 2010; revised manuscript received 27 October 2010; published 10 November 2010)

Recently bound states in vortex cores were observed by scanning tunneling microscopy measurement in iron pnictides. The local density of states $\rho(\omega,r)$ is asymmetrically peaked below the Fermi energy for $r=0$ (at the vortex core) and the peak splits and merges to the gap edges away from the vortex core ($r>0$). We performed exact large-scale calculation of the vortex-core electronic structure in effective lattice models with both in-phase s-wave (s_{++}) and antiphase s-wave (s_{+-}) pairing, and found results in qualitative agreement with the experiment. We argue that the peak energy ω_p is determined by the normal-state band structure, insensitive to the relative phase of the pairing gaps on the multiple bands. The observed bound state is compatible, although not exclusively, with s_{+-} pairing.

DOI: 10.1103/PhysRevB.82.184519 PACS number(s): 74.55.+v, 74.20.Pq, 74.20.Rp, 74.70.Xa

I. INTRODUCTION

Iron pnictides are a new family of high-temperature superconductors that have been the subject of extensive recent research (for example, see Refs. 1 and 2). Theoretically, since electron-phonon interaction does not seem to be strong enough to cause the high transition temperature,[3] pairing mechanism based on electron-electron interaction itself has been the focus of much attention. The multiband structure leads to disconnected Fermi pockets in the momentum space. Interpocket scattering is believed to first cause a spin-density-wave instability, and second by Luttinger-Kohn-type mechanism[4] (via higher order particle-hole processes) triggers a repulsive interpocket pair-scattering interaction, leading to antiphase s-wave (or s_{+-}) pairing gaps on the Γ and M pockets.[5–8] The same type of pairing also follows from some specific local-moment models,[9] which however has to be rectified against the apparent lack of Mott gap in iron pnictides. Clearly, the intrapocket pairing symmetry and perhaps more importantly the relative phase of the gap functions are the essential ingredients of electronic pairing mechanisms that have to be verified/falsified.[10–13] Experimentally, it seems that most pnictides have nodeless gaps,[14–16] compatible with s-wave pairing, except KFe_2As_2,[17] LaFePO,[18] and $BaFe_2As_{2-x}P_x$.[19] Neutron-scattering and phase-sensitive tunneling measurements are performed in search of the signature of s_{+-} pairing,[20,21] but consensus has not been achieved yet.

Recently, scanning tunneling spectroscopy (STM) measurements were performed on high-quality $Ba_{0.6}K_{0.4}Fe_2As_2$ samples in the mixed state.[22] In iron pnictides, clear Andreev bound states around the vortex core were observed. The local density of states (LDOS) $\rho(\omega,r)$ is asymmetrically peaked at ω_p below the Fermi energy for $r=0$ (at the vortex core), and the peak splits and merges to the gap edges away from the vortex core ($r>0$). The purpose of this work is to understand such features and uncover the connection, if any, to the pairing symmetry and the relative gap phase.

We performed exact large-scale calculation of the vortex core state with in-phase (s_{++}) and s_{+-} pairing, using a variety of tight-binding models. For both pairing symmetries, the calculated LDOS shows one peak at the core center, and the peak splits far away from the center and eventually merges to gap edges. The sign of the peak energy is however model dependent. In the simplest two-band model proposed in Ref. 23 (model A), ω_p is above the Fermi level, inconsistent with the STM result. In the two-band model proposed in Ref. 24 (model B), the three-band model proposed in Ref. 25 (model C), and the five-band model proposed in Ref. 7 (model D), ω_p is below the Fermi level, in agreement with STM result. The difference arises from the different band structures. In model A, the Fermi level is near the bottom of the electron pockets, while in model B, C, and D, it is near the top of one or several hole pockets. The sign of ω_p is negative/positive for hole/electron pocket edges. This difference is internally consistent by charge conjugation if only the shallow bands dominate the bound state. We therefore argue that the asymmetric bound state is due to the band edge effect and is therefore unfortunately insensitive to the relative phase of the pairing gaps. The observed bound state is compatible, although not exclusively, with s_{+-} pairing.

The rest of this paper is organized as follows. In Sec. II we discuss the vortex states within a simple one-band model. This is used to gain insights without the complication of multiband structure. In Sec. III, we discuss the vortex states within four different lattice models for iron pnictides. Finally Sec. IV contains the summary and discussion of the results.

II. ONE-BAND MODEL

As a digression and technical preparation, we first consider bound states in vortex cores of conventional s-wave superconductors. These bound states are marked by their magnetic quantum number ν (with 2ν an odd integer) and come in pairs with opposite energies (because of pairing). For small $|\nu|$, the energies of the bound states are equally spaced by $\Delta\omega\sim\Delta/k_F\xi$,[26–28] where Δ is the bulk gap, k_F the Fermi wave number, and ξ the coherence length. The guiding centers (the locus of the maximum wave-function amplitude) of such states are concentric circles around the vortex core and the guiding radius r_ω increases with increasing energy $|\omega|$. At a particular radial distance r, the contribution to LDOS comes mainly from the bound states with $r_\omega\sim r$. In the presence of small but finite smearing (due to thermal

effect or elastic scattering by impurities), the bound states lead to a zero-energy peak in LDOS for $r=0$ (the vortex-core position), and a pair of peaks at positive and negative energies for $r>0$. This cartoon-picture view summarizes the main results by quasiclassical Green's-function approaches.[29,30] However, implicit in such approaches is the assumption of a wideband with particle-hole symmetry, which is unable to capture the asymmetry under concern. On the other hand, the quasiclassical treatment requires $k_F\xi \gg 1$. In this limit, $\Delta\omega \ll \Delta$ so that the discrete levels would be easily smeared out by thermal energy and/or quasiparticle scattering. A better case can be made if ξ is on the order of the Fermi wavelength $2\pi/k_F$. In this case the Fermi level is close to the band edge within an energy scale of the pairing gap, and one has to go beyond the quasiclassical approximation and solve the problem exactly. Because of the importance of the band edge, the band structure is no longer symmetric with respect to the Fermi level within the gap energy scale, and nor would the bound states be. As a result, observable asymmetric bound states would appear, as found experimentally[31] and studied in a continuum model,[32] where such states were referred to as the quantum limit of the Caroli de Gennes states.

In the following we check whether the above picture manifests in lattice models. The purpose is threefold. First, we will use lattice models for the multiband iron pnictides. Second, in the above-mentioned quantum limit, the lattice model is better defined. Third, in the experimental situation, the intervortex distance is of the order of a few hundreds of the lattice constant. To mimic the situation we will consider an isolated vortex in an open $L\times L$ lattice system with large enough L. The large size reduces finite-size effect and also the overlap between core states from different vortices. However, with the large lattice (and also lack of knowledge of the pairing interaction for the pnictide models) we are unable to do self-consistent calculation for the vortex state. It is therefore important to check that an assumed profile for the vortex configuration is enough to reveal the bound states.

The lattice Hamiltonian can be written as

$$H = \sum_{i,j} \Psi_i^\dagger [-t_{ij}\sigma_3 - \mu\delta_{ij}\sigma_3 + (\Delta_i\delta_{ij}\sigma_+ + \text{H.c.})]\Psi_j, \quad (1)$$

where $\Psi_i = [c_{i\uparrow}, c_{i\downarrow}^\dagger]^T$ is the real-space Nambu spinor, $\sigma_+ = (\sigma_1 + i\sigma_2)/2$ and σ_3 are Pauli matrices, t_{ij} is the hopping integral, and Δ_i is the on-site pairing potential. In what follows we take $t_{ij}=t=1$ for nearest neighbors only and $\Delta_0 = 0.2$. We take the lattice constant $a=1$ and assume $\xi=10$ unless indicated otherwise. In principle, in the presence of a magnetic field t_{ij} should include a Peierls factor relating to the vector potential. However, for a dilute vortex lattice, we ignore this factor. This approximation is common[27] and in fact reliable in dealing with the vortex-core states. We consider an isolated vortex in an open $L\times L$ lattice with $L = 401$ in this section. The vortex is characterized by $\Delta_i = \Delta_0 \tanh(r_i/\xi)\exp(i\phi_i)$, where r_i (ϕ_i) is the radial distance (azimuthal angle) of a site i with respect to the core center.[33]

To calculate the LDOS around the vortex efficiently in our large lattice, we follow the real-space recursion method.[34,35] To be specific, the LDOS at site i is calculated as follows.

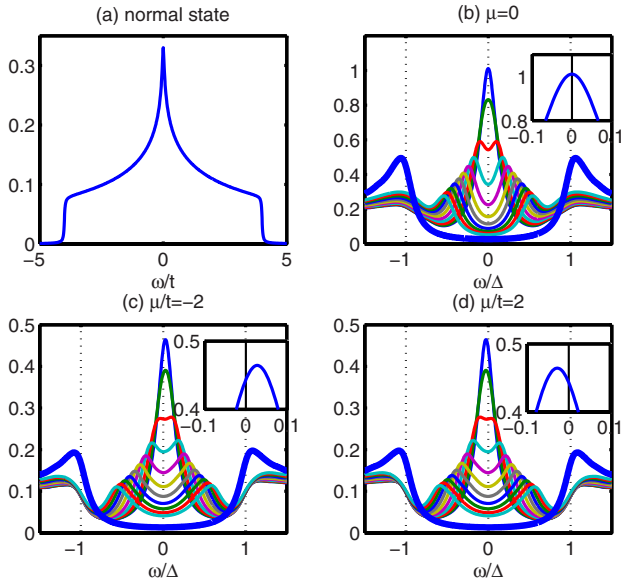

FIG. 1. (Color online) LDOS of the one band nearest-neighbor tight-binding model. (a) LDOS of normal state for $\mu=0$. (b) LDOS along a cut $(0,y)$ starting from the vortex core (thin lines). Viewing at zero energy, y increases by a successively from top to bottom. The thick line indicate the zero-field LDOS (or far from the vortex core). Here $\mu=0$. (c) The same plot as (b) but for $\mu=2$. (d) The same plot as (b) but for $\mu=-2$. The insets in (b)–(d) blow up the low-energy peaks.

We take the single-particle state $c_{i\uparrow}^\dagger|0\rangle$, where $|0\rangle$ is the vacuum with no electrons, as an initial state and apply the standard Lanczos method to convert the single-particle Hamiltonian to a tridiagonal matrix with $\{a_k; k=0,\ldots,K\}$ and $\{b_k; k=0,\ldots,K-1\}$ as the diagonal and subdiagonal elements, respectively. Here K is the optimal size of the Lanczos chain. Then the retarded local Green's function (suitable for $c_{i\uparrow}$) at site i is given by a continued fraction,

$$G(\omega,i) = \cfrac{1}{\omega + i\eta - a_0 - \cfrac{b_0^2}{\omega + i\eta - a_1 - \cfrac{b_1^2}{\cdots}}}, \quad (2)$$

where η is a suitable smearing factor, on the order of t/L, which effectively reduces finite-size effect. Finally the LDOS is obtained as $\rho(\omega,i) = -\text{Im}\, G(\omega,i)/\pi$.

As a reference, Fig. 1(a) shows the normal state DOS for $\mu=0$. There is a Van Hove singularity in the band center. By tuning μ the Fermi level is either close to the bottom or the top of the band. In the vortex state, we first present the LDOS in the symmetric case ($\mu=0$) in Fig. 1(b). We see a zero-bias peak at the vortex-core center and the peak splits along the cut away from the core (thin lines). Far from the core the peaks merge to the gap edges and the curve evolves to the zero-field one (thick line). These qualitative features are in line with the above-mentioned cartoon picture and are known from other techniques.[30,36,37] Figures 1(c) and 1(d) are the same plots as Fig. 1(b), except that $\mu=\pm 2$ in (c) and (d), respectively. The sign of ω_p, as highlighted in the insets,

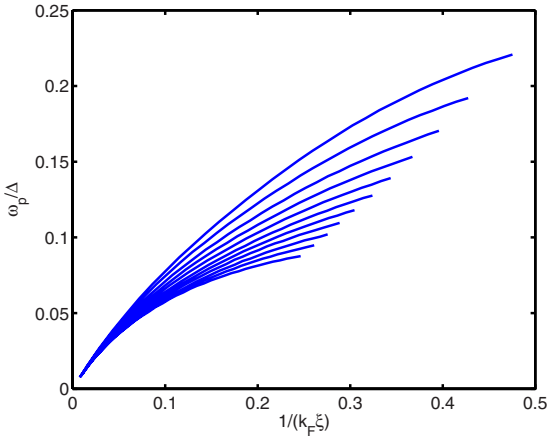

FIG. 2. (Color online) The peak energy ω_p as a function of $1/k_F\xi$. From top to bottom, $\mu=-3.0,-2.8,\ldots,-1.0$.

is negative (positive) for $\mu=2$ ($\mu=-2$), in line with the position of the Fermi level with respect to the band edges.

To see the systematics we performed calculation of the LDOS for a range of μ and ξ. The peak energy as a function of $1/k_F\xi$ is shown in Fig. 2 for $\mu=-3.0,-2.8,\ldots,-1.0$ from top to bottom. Here $\omega_p>0$ since the Fermi level is closer to the bottom of the band in the cases considered. We see that the curves merge together in the limit $1/k_F\xi\ll 1$, confirming the results in the quasiclassical limit. For large $1/k_F\xi$, the magnitude of ω_p is larger if the Fermi level is closer to the band bottom (or for more negative μ). This result is in agreement with the continuum model in the same limit[32] and validates the assumptions we made for the vortex states.[33]

III. MULTIBAND MODELS FOR IRON PNICTIDES

A. Model A

Having understood the origin of the nonzero bias peak, we now consider model A, a simplest two-band model proposed in Ref. 23 for the iron pnictides. The Hamiltonian is written as

$$H=\sum_{ia,jb}\Psi^{\dagger}_{ia}[t_{ia,jb}\sigma_3-\mu\delta_{ij}\delta_{ab}\sigma_3+(\Delta_{ij}\delta_{ab}\sigma_+ + \text{H.c.})]\Psi_{jb}, \tag{3}$$

where i and j are site indices, and a and b are orbital indices. In the present two-orbital case a or b runs over the xz and yz orbitals. We adopt the hopping integrals suggested in Ref. 23 for $t_{ia,jb}$ and set $\mu=1.45$ to produce a right topology of the Fermi pockets. The pairing is assumed to occur between identical orbitals since nodal gap would appear otherwise according to a group theoretical analysis.[38] We consider two typical s-wave pairing cases. For the s_{++} case we assume electrons pair on-site wise, leading to a uniform gap everywhere in the momentum space (in the absence of vortices). For the s_{+-} case we assume electrons pair on next-nearest-neighboring sites, leading to a gap form factor $\cos k_x \cos k_y$ in the momentum space, which changes sign from the hole pocket to the electron pocket. Similar to the one-band case, the vortex here is characterized by $\Delta_{ij}=\Delta_0\tanh(r_{ij}/\xi)\exp(i\phi_{ij})$ in which r_{ij} is radial center-of-mass position of the electron pair, and ϕ_{ij} is the associated azimuthal angle.[33] A 401×401 lattice is used in the following calculations.

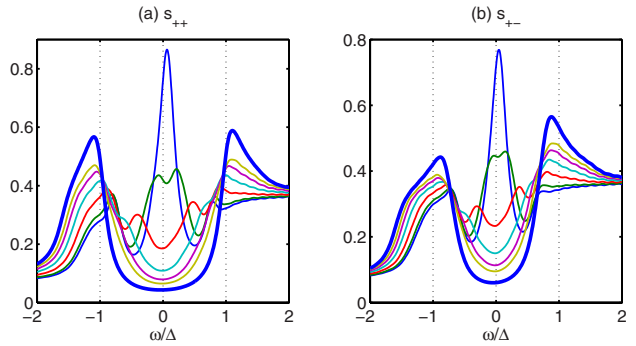

FIG. 3. (Color online) LDOS of model A with (a) s_{++} and (b) s_{+-} pairing along a line cut $(0,y)$ starting from the vortex-core center. Viewing at zero energy, y increases by $2a$ successively from top to bottom. The thick line indicates the bulk LDOS.

The LDOS in the vortex states is presented in Fig. 3. Since the general feature does not depend on the orbital character in this case, only the total LDOS, an equal-weight sum of the contributions from both orbitals are shown. In both (a) s_{++} and (b) s_{+-} cases, we find a nonzero ω_p above the Fermi level at the vortex-core center (top line).[39,40] While the following peak splitting and merging to the gap edge as we move away from the vortex core center is in agreement with the STM result, the sign of ω_p disagrees. Moreover, a comparison between Figs. 3(a) and 3(b) shows that the general features of the vortex-core states are indifferent to the relative phase of the pairing gaps.

To check whether the band edge effect found in the one-band model preserves in the multiband case, we also performed calculations for μ in the whole band range (for s_{++} pairing only, given the indifference of ω_p to the two types of s-wave pairing). In Figs. 4(a) and 4(b), we plot the band-structure and normal-state DOS. We find that the Fermi level used in Fig. 3 is just above the band bottom near $(\pi,0)$ and a positive ω_p seems to be consistent with the band-edge effect in the one-band case. In Fig. 4(c), we plot a series of LDOS curves at the vortex-core center, vertically shifted for clarity. We see that the magnitude of ω_p is particularly large at $\mu\sim-8$, 1.2, and 4 (marked by A, B, and C, respectively, in Fig. 4) where the Fermi level is near the bottom or top of the bands within the gap energy scale. The sign of ω_p is also in agreement with the band-edge effect found in the one-band model.

Therefore, the wrong sign of ω_p in Fig. 3 (as compared to the experimental one) is clearly an artifact of this model. Although it produces Fermi pockets in qualitative agreement with the local-density approximation (LDA) band structure after folding the Brillouin zone, the Fermi level is close to the bottom of the electron pockets, as shown in Fig. 3(a), in contrast to the LDA band structure.

B. Model B

We now consider another two-orbital model proposed in Ref. 24 (model B). This model breaks the A-B lattice sym-

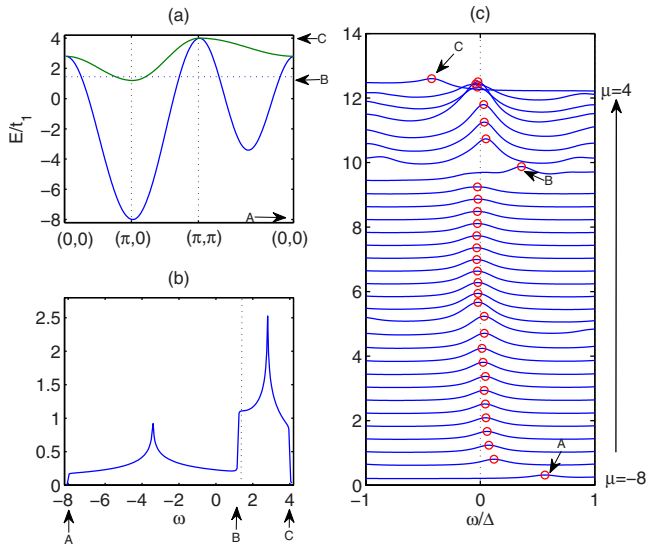

FIG. 4. (Color online) (a) Band structure of model A plotted along high-symmetry cuts $(0,0)\rightarrow(\pi,0)\rightarrow(\pi,\pi)\rightarrow(0,0)$ in the unfolded Brillouin zone. The Fermi level ($\mu=1.45t_1$) of undoped sample is marked by the dotted line. (b) LDOS in the normal state. The energy is in units of t_1. (c) LDOS at the vortex-core center for on-site pairing. The lines are vertically shifted for clarity. From top to bottom, $\mu=4,3.6,3.2,\ldots,-8$ (eV). The positions of nonzero bound states are marked by open circles. $\mu=-8$, 1.2, and 4 are marked by text arrow A, B, and C respectively.

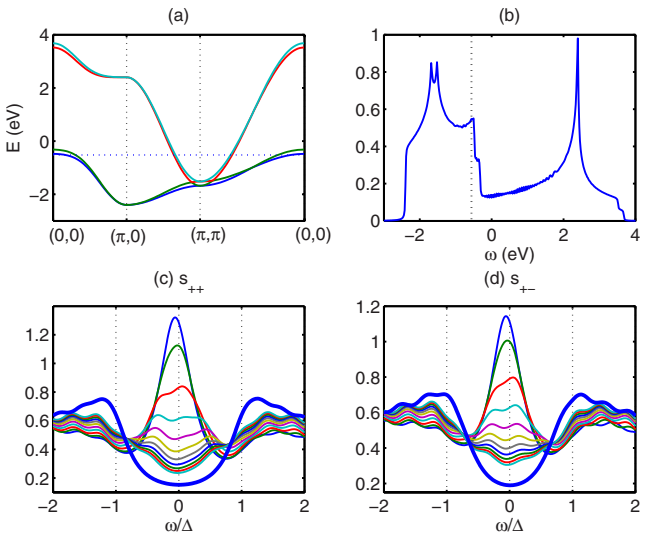

FIG. 5. (Color online) Results of model B. (a) Band structure plotted along $(0,0)\rightarrow(\pi,0)\rightarrow(\pi,\pi)\rightarrow(0,0)$ defined in folded BZ. (b) DOS in the normal state. The Fermi level used in calculation are marked by dotted lines in both (a) and (b). (c) Total LDOS along a line cut $(0,y)$ starting from the vortex-core center for the case of s_{++} pairing. Viewing at zero energy, y increases by $3a$ successively from top to bottom. The thick line indicates the bulk LDOS. (d) The same as (c) but for s_{+-} pairing.

metry and is subject to some debate.[41] However, it reproduces two hole pockets that are nondegenerate at the zone center, in better agreement with angle resolved photoemission spectroscopy. Therefore it might be a suitable effective model. For the parameters we refer to Ref. 24. The setting of the pairing potential is the same as in model A. The band structure is shown in Figs. 5(a) and 5(b), for $\mu=-0.512$ eV, which yields a reasonable doping level and Fermi-surface topology. The band structure is very different from model A. The Fermi level is close to the top of the hole band at (0,0). The DOS is also very different. According to the band-edge effect we would expect opposite sign of ω_p in these two models. This is indeed the case. For both s_{++} [Fig. 5(c)] and s_{+-} [Fig. 5(d)], there is a nonzero-bias peak below the Fermi level ($\omega_p<0$) at the vortex-core center, splitting far away from the center, and eventually merging to the gap edges, in qualitative agreement with the STM data.[22] The magnitude of ω_p is relatively small for $\xi=10$ in our calculation but it could be tuned larger for smaller ξ.

C. Model C

Next we consider a more sophisticated three-band model, model C, for the iron pnictides. The purpose is twofold. First, a three-band provide a more faithful approximation to the LDA band structure. Second, we use this model to check whether the band-edge effect survives with more bands. We use the tight-binding model proposed in Ref. 25. The model includes the xz, yz, and xy orbitals. The results are presented in Fig. 6. The Fermi level is marked by the dotted line in Figs. 6(a) and 6(b). It is also near the top of the hole bands.

The bound state energy ω_p is negative as seen in the LDOS near the vortex core, as shown in Figs. 6(c) and 6(d), for s_{++} and s_{+-} pairing, respectively. The evolution of the LDOS along the cut is similar to that in model B and the asymmetric peak is also insensitive to the s-wave pairing symmetries.

D. Model D

Finally we consider the five-band models which respect the LDA band structure most comprehensively.[7,42–44] With many bands or orbitals, the pairing amplitude may strongly

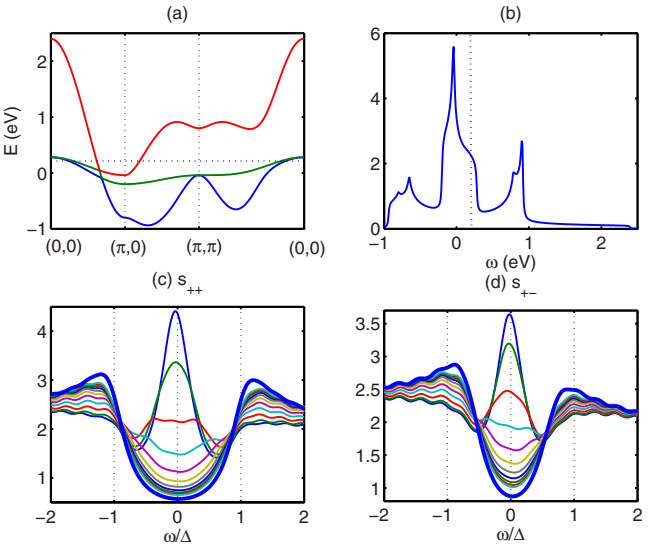

FIG. 6. (Color online) The same plot as Fig. 5 but for model C.

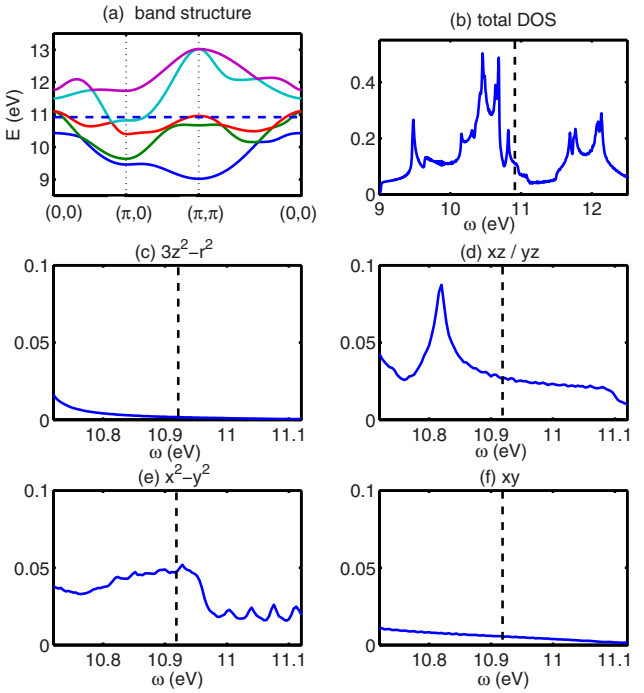

FIG. 7. (Color online) Band structure and DOS of the normal state of the five-orbital model. (a) Band structure of the five-orbital model, plotted along the path $(0,0)\rightarrow(\pi,0)\rightarrow(\pi,\pi)\rightarrow(0,0)$. (b) The total DOS of five orbitals. (c)–(f) are orbital-resolved DOS. The degenerate xz and yz orbitals are plotted in the same panel. The dashed lines in all panels indicate the Fermi level.

depend on the band. In the absence of a clear understanding of the pairing interaction in such sophisticated models, the band-dependent amplitudes cannot be resolved. Leaving band- or orbital-dependent pairing potential for further study, in the following we take the same assumption on the pairing potential as in previous models for the simplest purpose. The Hamiltonian now contains five orbitals, namely, the $3z^2-r^2$, xz, yz, xy, and x^2-y^2 orbitals. We adopt the hopping integrals proposed in Ref. 7 and set $\mu=10.92$ eV to yield a reasonable doping level. The band structure and the total DOS are presented in Figs. 7(a) and 7(b). We remark that at this doping level there are in fact three hole pockets in the folded Brillouin-zone center which is different from models A, B, and C. Because of strong orbital dependence, we also show the normal-state orbital-resolved DOS in Figs. 7(c)–7(f). To enhance numerical resolution but without loss of generality, we use a larger gap size $\Delta=0.02$ eV and a smaller coherence length $\xi=5a$. The lattice size is still 201×201.

The LDOS for the s_{++} and s_{+-} cases are shown in Figs. 8 and 9, respectively. Since the five orbitals contribute unevenly, we present orbital-resolved LDOS in panels (a)–(c) in these figures for xz/yz, x^2-y^2, and xy channels, respectively. (The $3z^2-r^2$ channel is not shown since its contribution is one or two orders of magnitude smaller than the others.) The evolution of the LDOS along the cut is similar to the other models. At the vortex-core center ($y=0$), the asymmetry of the peaks are apparent in the x^2-y^2 and xy orbitals, but is barely visible in the xz and yz channels. This can be understood in terms of the band-edge effect as follows. From

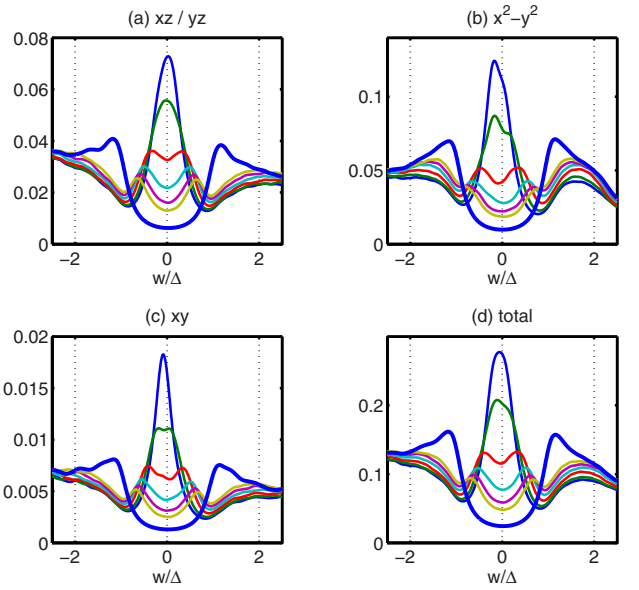

FIG. 8. (Color online) LDOS of the five-orbital model along a cut $(0,y)$ for s_{++} wave pairing. (a)–(c) show the LDOS in the xz/yz, x^2-y^2, and xy channels, respectively, and (d) is the equal-weight sum of all orbitals. Viewing at zero energy, y increases by $3a$ successively from top to bottom. The thick lines indicate the bulk LDOS.

Fig. 7(a) the Fermi level is near the tops (bottoms) of the hole (electron) pockets. By further inspection of the distribution of the orbital characters on the Fermi pockets (not shown here), we find that the x^2-y^2 and xy orbitals contribute closed (π,π) and (0,0) pockets, respectively, yielding the negative peaks in these two channels. On the other hand, the xz and yz orbitals contributes to both electron pockets and disconnected (0,0)-hole pockets. Moreover the band bottom and top are nearly symmetric with respect to the Fermi level. This leads to cancellation in the asymmetry. In Figs. 8(f) and

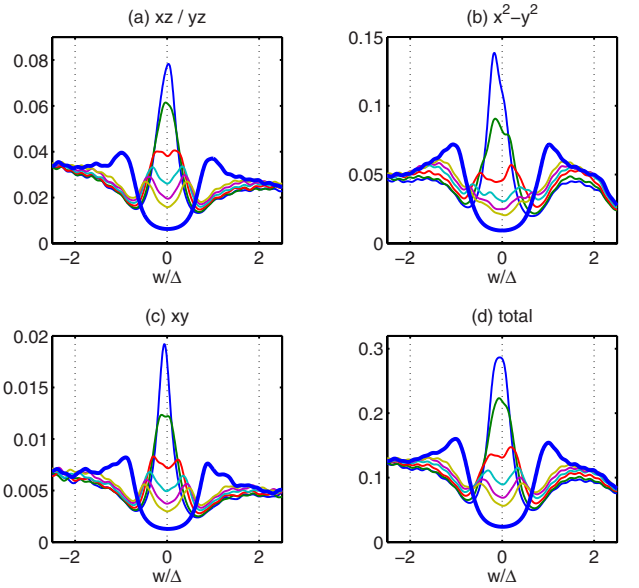

FIG. 9. (Color online) The same plot as Fig. 8 but for s_{+-} pairing.

9(f), we add the contributions of all of the five orbitals directly. The asymmetry is resolvable and the evolution of the peak structure along the cut is in qualitative agreement with the STM results. However, a quantitative comparison between theory and experiment would be difficult since in STM the tunneling matrix element might require significant orbital dependence.

We conclude that the band-edge effect holds in all of the four models considered so far, and that models B, C, and D provide results in qualitative agreement with the STM results since in these models the Fermi level is near the top of at least one hole band. While it is insensitive to the relative phase of the pairing gaps, the asymmetric peak does favor models B, C, and D instead of A.

IV. SUMMARY AND DISCUSSION

To summarize, by exact large-scale calculation of the vortex-core state with s_{++} or s_{+-} pairing, we find a bound state LDOS peak at the core center, which splits away from the center and eventually merges to gap edges. The sign of the peak energy is positive/negative if the Fermi level is near the bottom/top of the electron/hole bands but turns out to be insensitive to the relative phase of the pairing gaps. In the four models considered for the iron pnictides, models B, C, and D produces results consistent with the STM results. We therefore argue that the asymmetric bound state is due to the band-edge effect. The observed bound state is compatible, although not exclusively, with s_{+-} pairing.

According to the band-edge effect, the nonzero vortex-core bound states, observed in $Ba_{0.6}K_{0.4}Fe_2As_2$,[22] should also be observed in $Ba(Fe_{1-x}Co_x)_2As_2$ if the system is in the clean limit, since by electron doping the Fermi level would be closer to the top of the hole bands. However, Co doping into FeAs layers, although provides charge carriers to achieve superconductivity, it also introduces in-plane scattering centers. Therefore, the bound states could be smeared out in the vortices of $Ba(Fe_{1-x}Co_x)_2As_2$ (Ref. 45) while survive in the off-plane doped $Ba_{0.6}K_{0.4}Fe_2As_2$.

During resubmission of this paper we became aware of a related work[46] addressing similar issues but using a vortex lattice with an intervortex distance of 24 Fe-Fe lattice constant. The dense vortices lead to double peaks at each core center, possibly because of overlapping core states.

ACKNOWLEDGMENTS

The work was supported by NSFC under Grants No. 10974086 and No. 10734120, the Ministry of Science and Technology of China (under Grants No. 2006CB921802 and No. 2006CB601002), and the 111 Project (under Grant No. B07026).

*qhwang@nju.edu.cn

[1] I. I. Mazin, Nature (London) **464**, 183 (2010).
[2] D. C. Johnston, Adv. Phys. **59**, 803 (2010).
[3] L. Boeri, O. V. Dolgov, and A. A. Golubov, Phys. Rev. Lett. **101**, 026403 (2008).
[4] W. Kohn and J. M. Luttinger, Phys. Rev. Lett. **15**, 524 (1965).
[5] I. I. Mazin, D. J. Singh, M. D. Johannes, and M. H. Du, Phys. Rev. Lett. **101**, 057003 (2008).
[6] A. V. Chubukov, D. V. Efremov, and I. Eremin, Phys. Rev. B **78**, 134512 (2008).
[7] K. Kuroki, S. Onari, R. Arita, H. Usui, Y. Tanaka, H. Kontani, and H. Aoki, Phys. Rev. Lett. **101**, 087004 (2008).
[8] F. Wang, H. Zhai, Y. Ran, A. Vishwanath, and D. H. Lee, Phys. Rev. Lett. **102**, 047005 (2009).
[9] K. Seo, B. A. Bernevig, and J. P. Hu, Phys. Rev. Lett. **101**, 206404 (2008).
[10] J. S. Wu and P. Phillips, Phys. Rev. B **79**, 092502 (2009).
[11] D. Wang, Y. Wan, and Q. H. Wang, Phys. Rev. Lett. **102**, 197004 (2009).
[12] W. Q. Chen, F. J. Ma, Z. Y. Lu, and F. C. Zhang, Phys. Rev. Lett. **103**, 207001 (2009).
[13] E. Plamadeala, T. Pereg-Barnea, and G. Refael, Phys. Rev. B **81**, 134513 (2010).
[14] H. Ding, P. Richard, K. Nakayama, K. Sugawara, T. Arakane, Y. Sekiba, A. Takayama, S. Souma, T. Sato, and T. Takahashi, EPL **83**, 47001 (2008).
[15] T. Kondo, A. F. Santander-Syro, O. Copie, C. Liu, M. E. Tillman, E. D. Mun, J. Schmalian, S. L. Budko, M. A. Tanatar, P. C. Canfield, and A. Kaminski, Phys. Rev. Lett. **101**, 147003 (2008).
[16] T. Y. Chen, Z. Tesanovic, R. H. Liu, X. H. Chen, and C. L. Chien, Nature (London) **453**, 1224 (2008).
[17] J. K. Dong, S. Y. Zhou, T. Y. Guan, H. Zhang, Y. F. Dai, X. Qiu, X. F. Wang, Y. He, X. H. Chen, and S. Y. Li, Phys. Rev. Lett. **104**, 087005 (2010).
[18] J. D. Fletcher, A. Serafin, L. Malone, J. G. Analytis, J. H. Chu, A. S. Erickson, I. R. Fisher, and A. Carrington, Phys. Rev. Lett. **102**, 147001 (2009).
[19] Y. Nakai, T. Iye, S. Kitagawa, K. Ishida, S. Kasahara, T. Shibauchi, Y. Matsuda, and T. Terashima, Phys. Rev. B **81**, 020503 (2010).
[20] A. D. Christianson, E. A. Goremychkin, R. Osborn, S. Rosenkranz, M. D. Lumsden, C. D. Malliakas, I. S. Todorov, H. Claus, D. Y. Chung, M. G. Kanatzidis, R. I. Bewley, and T. Guidi, Nature (London) **456**, 930 (2008).
[21] C. T. Chen, C. C. Tsuei, M. B. Ketchen, Z. A. Ren, and Z. X. Zhao, Nat. Phys. **6**, 260 (2010).
[22] L. Shan, Y. L. Wang, B. Shen, B. Zeng, Y. Huang, Y. Xuan, D. Wang, H. Yang, C. Ren, S. H. Pan, Q. H. Wang, and H. H. Wen, arXiv:1005.4038 (unpublished).
[23] S. Raghu, X. L. Qi, C. X. Liu, D. J. Scalapino, and S. C. Zhang, Phys. Rev. B **77**, 220503 (2008).
[24] D. G. Zhang, Phys. Rev. Lett. **103**, 186402 (2009).
[25] M. Daghofer, A. Nicholson, A. Moreo, and E. Dagotto, Phys. Rev. B **81**, 014511 (2010); Another three-band model (not used in this paper) can be found in, e.g., P. A. Lee and X. G. Wen, *ibid.* **78**, 144517 (2008).
[26] C. Caroli, P. G. De Gennes, and J. Matricon, Phys. Lett. **9**, 307

(1964).
[27] P. G. de Gennes, *Superconductivity of Metals and Alloys* (Addison-Wesley, Reading, 1966).
[28] J. Bardeen, R. Kummel, A. E. Jacobs, and L. Tewordt, Phys. Rev. **187**, 556 (1969).
[29] S. Ullah, A. T. Dorsey, and L. J. Buchholtz, Phys. Rev. B **42**, 9950 (1990).
[30] U. Klein, Phys. Rev. B **40**, 6601 (1989).
[31] H. Nishimori, K. Uchiyama, S.-i. Kaneko, A. Tokura, H. Takeya, K. Hirata, and N. Nishida, J. Phys. Soc. Jpn. **73**, 3247 (2004).
[32] N. Hayashi, T. Isoshima, M. Ichioka, and K. Machida, Phys. Rev. Lett. **80**, 2921 (1998).
[33] The phase winding of the vortex is unique up to trivial gauge transforms. On the other hand, in self-consistent calculations, the vortex potential well might be slightly noncircular, particularly in the subdominant channel of a model with competing pairing order parameters, see, e.g., Y. Ren, J. H. Xu, and C. S. Ting, Phys. Rev. Lett. **74**, 3680 (1995); Q. H. Wang and Z. D. Wang, Phys. Rev. B **54**, R15645 (1996). However, we are addressing *s*-wave pairing models without subdominant channels. Moreover, even a slightly noncircular vortex profile should only lead to insignificant difference to the bound states since the latter follow from the topological phase winding of the pairing order parameter.
[34] E. R. Gagliano and C. A. Balseiro, Phys. Rev. Lett. **59**, 2999 (1987).
[35] M. Cheng and W. P. Su, Phys. Rev. B **72**, 094512 (2005).
[36] J. D. Shore, M. Huang, A. T. Dorsey, and J. P. Sethna, Phys. Rev. Lett. **62**, 3089 (1989).
[37] F. Gygi and M. Schluter, Phys. Rev. B **41**, 822 (1990).
[38] Y. Wan and Q. H. Wang, EPL **85**, 57007 (2009).
[39] X. Hu, C. S. Ting, and J. X. Zhu, Phys. Rev. B **80**, 014523 (2009).
[40] H.-M. Jiang, J.-X. Li, and Z. D. Wang, Phys. Rev. B **80**, 134505 (2009).
[41] M. Daghofer and A. Moreo, Phys. Rev. Lett. **104**, 089701 (2010); D. Zhang, *ibid.* **104**, 089702 (2010).
[42] C. Cao, P. J. Hirschfeld, and H.-P. Cheng, Phys. Rev. B **77**, 220506(R) (2008).
[43] V. Cvetkovic and Z. Tesanovic, EPL **85**, 37002 (2009).
[44] M. J. Calderón, B. Valenzuela, and E. Bascones, Phys. Rev. B **80**, 094531 (2009).
[45] Y. Yin, M. Zech, T. L. Williams, X. F. Wang, G. Wu, X. H. Chen, and J. E. Hoffman, Phys. Rev. Lett. **102**, 097002 (2009).
[46] Y. Gao, H. X. Huang, C. Chen, C. S. Ting, and W. P. Su, arXiv:1008.3885 (unpublished).